

# **MODIFICATIONS TO STRUCTURED PACKINGS TO INCREASE THEIR CAPACITY**

**Peter Bender, Anton Moll**

LINDE AG, 82049 Höllriegelskreuth / Munich, Germany

## **ABSTRACT**

The hydraulic performance of structured packed columns is characterised by parameters such as loading point, flooding point, dry and wet pressure-drop. These parameters can be positively influenced by optimising the transition areas between two adjacent packing layers. Tests have been done in a two-phase test rig with a rectangular column made of perspex. The test medium is a liquid hydrocarbon in counterflow to saturated nitrogen gas. The performance of different packing structures at the layer-to-layer transition zone and the addition of vane-type elements between two packing layers was evaluated. Several packing modifications were tested and the results were compared with those of a non-modified packing. The intentions of this work are:

- to rank the modifications of structured packings with respect to the achieved capacity increase
- to determine whether flooding is initiated in the core of the corrugated packing or in the transition area in spite of the modifications made on the lower or top side of the packing sheets
- to find out how the loading point is influenced by the modifications

## **INTRODUCTION**

For more than ten years, Linde AG has been manufacturing structured packings for use in air separation plants. In air separation, the use of dense packing is common because of the need to reduce the height of the cold box caused by the very large number of theoretical trays needed for the separation of N<sub>2</sub>, Ar and O<sub>2</sub>. A great part of the packing produced by Linde therefore has a specific surface area of 750 m<sup>2</sup>/m<sup>3</sup>, designation Linde Type A750Y.

To reduce the investment costs for the columns, capacity has to be increased without reducing the efficiency or the efficiency has to be increased without reducing capacity -or both.

Although means of improving the capacity of a structured packing have been known for many years, some simple but effective changes in the packing geometry have been employed recently. Many of these modifications refer to the optimisation of the design at the interface zone between two packing layers. For example, Sulzer offers the Mellapak Plus, a packing with vertical bent corrugations at the top and bottom side of the packing sheets. Koch Glitsch produces the FLEXIPAK-HC with the bottom edge of the sheet elements flattened to a height of approximately 12 mm [1]. However, the only way to find the most beneficial geometry modification is to make each of the modifications in turn with the same packing geometry in the core and test under the same conditions. In this work, we investigated the following geometry changes to the type A750Y packing:

- height-staggered packing sheets
- different types of lattice grid between adjacent packing layers
- packing sheets with different flattened ends on the bottom part, similar to the Koch-Glitsch FLEXIPAC-HC, with both ends flattened, and with only the top end flattened
- packing sheets, in which the corrugation on the bottom and top part is bent vertically, similar to the Sulzer MELLAPAK-PLUS
- packing sheets in which only the bottom part of the corrugations is bent vertically, similar to the Montz B1-M series.

To investigate the effect of the liquid load on the achievable capacity increase, different loads up to  $30\text{m}^3/\text{m}^2\cdot\text{hr}$  have been tested.

Pressure drop and capacity have been compared with a conventional Linde packing A750Y. The tendency of the investigated geometry changes to generate maldistribution certainly varies from type to type and will have an influence on the efficiency – this is, however, not covered in this work.

## **EXPERIMENTAL**

The capacity measurements were made in our rectangular hydraulic test column. This 400mm x 400mm column is made from perspex to allow visual observation. The maximum possible packed height is 900mm.

Our test system uses a low boiling point hydrocarbon as liquid phase. It is non-polar, low-toxic and has a low surface tension. The gas phase is nitrogen saturated with the liquid component. The physical properties of this system at room temperature correspond approximately to those of liquefied air and therefore allow reliable hydraulic predictions. The physical properties are displayed in Table 1.

Table 1: Properties of the test system at atmospheric pressure and ambient temperature

Substance (at T=20°C)	Density [kg/m <sup>3</sup> ]	dyn. Viscosity [N·sec/m <sup>2</sup> ]	Surface tension [N/m]
Low boiling point hydrocarbon (LBH)	650	0.31·10 <sup>-3</sup>	18·10 <sup>-3</sup>
Hydrocarbon saturated nitrogen gas	1.7	0.12·10 <sup>-4</sup>	--

The test rig has been described in detail by Ranke et al. [6]. Briefly, the system works at 1.1bar and a controlled ambient temperature so allowing adiabatic tests. For each of the tested packing modifications four packing layers with a total height of 0.82m are installed, being cut exactly to 400mm x 400mm blocks to fit closely into the column. No wall wipers are used. The packing is supported by a lattice grid with 3 x 20mm bars and 91,5% free area. The liquid phase is fed to the top of the packing by a pipe distributor with a drip point density of 237/m<sup>2</sup>.

### PARAMETERS THAT INFLUENCE THE CAPACITY

There are several mechanistic pressure drop models [6, 7, 8] in the literature, describing the different contributions to the total pressure drop. All of them need parameters to fit the calculations to the measured pressure drop especially above the loading region – this leads to a striking increase in pressure drop and hold up. These models are therefore hardly helpful in understanding the influence of geometry changes at the layer to layer transition zone.

In their investigation of hold-up in structured packed columns, Suess and Spiegel [3] showed that flooding starts at the horizontal interface between two packing layers in structured packing. About half of the pressure drop in a layer occurs in this transition zone [5].

The sudden lack of surface area for the liquid trickling down is responsible for a liquid build up at the bottom of the sheets. The area at the contact points is only a few percent of the area above. As the packing layers are rotated 90° to each other, this cannot be avoided.

Another reason for the build up of liquid at the transition zone is the shearing force the gas exerts on the interface area between the liquid and gas. The sudden directional change of 60° at the transition between two packing layers causes separation and an additional constriction in the gas flow.

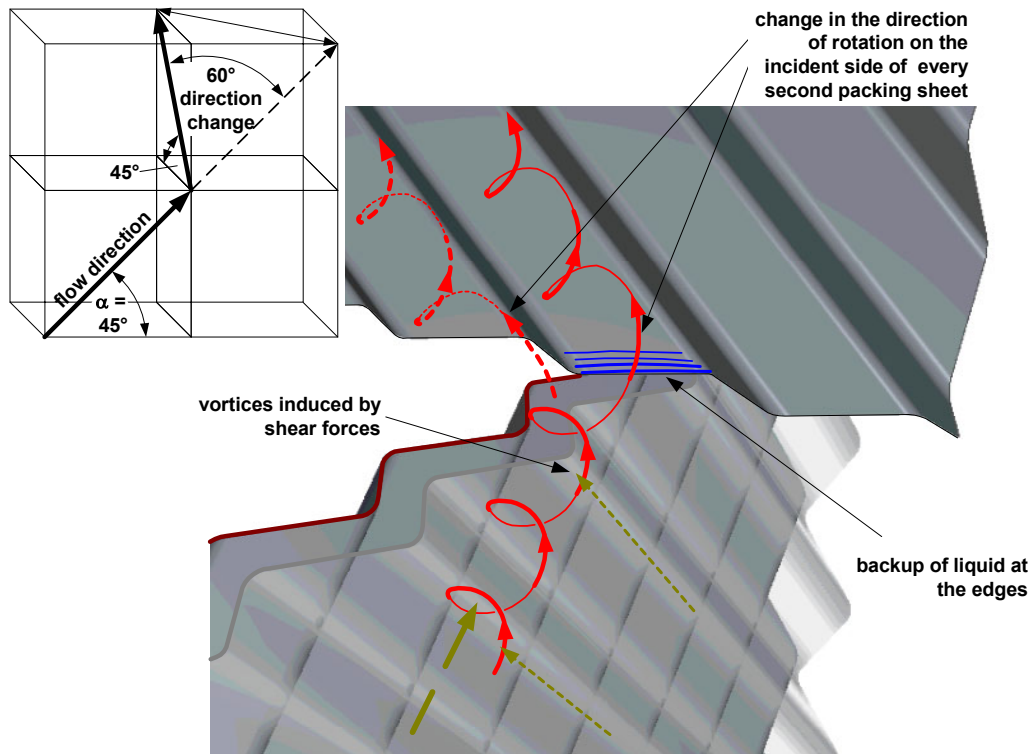


Figure 1: Packing geometry at the transition from one packing layer to a layer below. Shown is one packing sheet above and two sheets below. The first sheet is translucent. Vortices in the gas flow are induced due to shear forces. The liquid film thickens at the lower edge of the sheets. Above the load point a bubbling layer builds up. For every second sheet the angular momentum of the gas flow vortices changes the direction.

Figure 1 depicts the geometry at the transition zone of two layers and Figure 2 the constriction of the gas velocity profile.

The shearing force depends on the effective gas velocity in the entrance area to the gas channel. The interface area is proportional to the flow channel circumference. Reducing the effective gas velocity and or the circumference will therefore shift the onset of loading to a higher throughput. The loading point strongly influences the packing capacity.

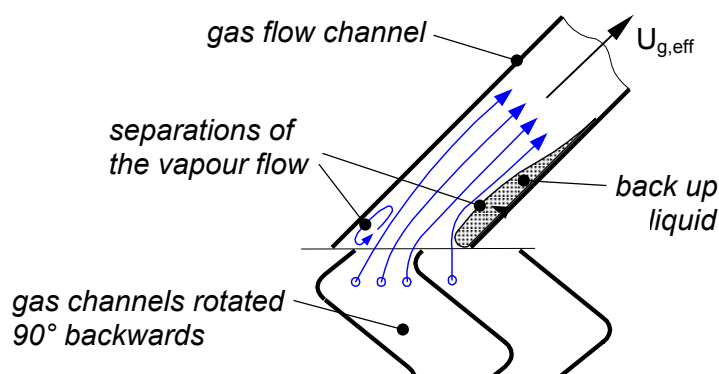


Figure 2: Schematic diagram of the gas flow constriction at the entrance to the lower side of the packing layer. The velocity profile at the entrance is disturbed because of a sharp change in direction between the flow channels below and above and because of a liquid back up.

Visual observation of the liquid flowing from one sheet to the sheet below is difficult due to the small corrugation channels of our packing A750Y. Verschoof et al. [9] suggest that only a small part of the descending liquid reaching the bottom edge of the packing sheet runs immediately to the top of the sheet just below. The transition takes place at the contact point of the sheets. In the zone where the sheet edge is above the empty space of the gas flow channel, the descending liquid pours onto the surface of the flow channels below, forming a curtain of liquid disrupted by the gas flow. We were not able to observe this pouring phenomenon. Probably the liquid film thickens up to a value where a balance between the draining flow to the sheets below and the thickened film is reached.

Verschoof et al. [9] developed an empirical correlation for the prediction of the loading point of corrugated sheet structured packings applicable for liquid loads up to 50 m<sup>3</sup>/m<sup>2</sup>·hr. For constant liquid load the gas load factor  $F_G$  depends among other things, on the geometric parameters void fraction  $\varepsilon$ , hydraulic diameter  $d_{hG}$  and the corrugation inclination angle  $\alpha$ .

$$F_G \cong \left[ \varepsilon^2 * d_{hG} * \sin(\alpha)^{1.24} \right]^{0.57} \quad (1)$$

The correlation was developed for homogenous packings and is therefore not fully applicable to our tests. For example the corrugation angle is not defined for flattened edges or for height-staggered sheets in the modified part.

We found that the packing geometry at the lower part of the packing sheets is the determining factor for the capacity. An application of the formula to this part roughly indicates the influence on the possible capacity increase. According to this formula, doubling the hydraulic diameter increases the gas load factor by up to 148%. Increasing the corrugation angle  $\alpha$  from 45° to 90° increases the  $F_G$  to 128%. The measured capacity increase for sheets with a bend at the bottom part decreases with increasing liquid load. For example (Figure 12) at a liquid load of 8m<sup>3</sup>/m<sup>2</sup>·hr the increase is 138%. Looking at the longer corrugation base length (by a factor 1/sin( $\alpha$ ), caused by bending the corrugation to the vertical) which enlarges the hydraulic diameter by 9%, an increased  $F_G$  for the load point of 134% is calculated in good agreement with the measured value.

## MODIFICATIONS TESTED TO INCREASE THE CAPACITY

Basis of our tests was a Linde packing A750Y with a specific surface area of 750 m<sup>2</sup>/m<sup>3</sup> and a corrugation inclination angle of 45°. The packing is made from 0.2mm-thick aluminium sheets. The surface is fluted.

For some of the tests with a flattened edge and for the tests with a bend in the corrugation the type A750-PA was used. In this type, the corrugation ridges have a smaller radius.

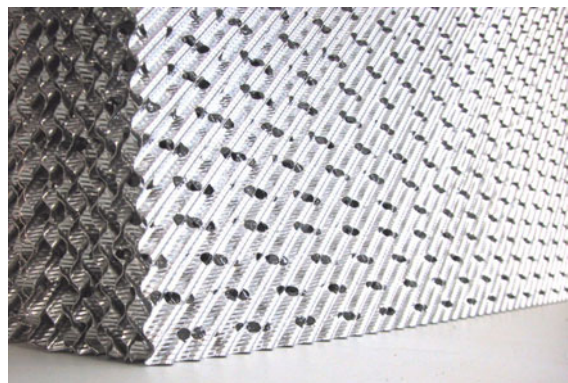


Figure 3: Linde aluminium packing A750Y

A first series of tests was made with three different vane type elements between the adjacent packing layers as shown in Figure 4. These elements reduce the change in the gas flow direction from 60° to 45°.

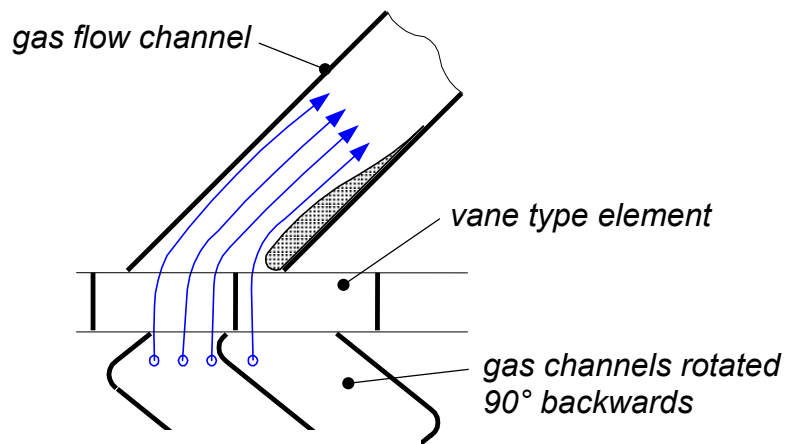
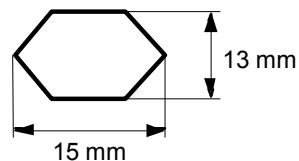


Figure 4: vane type element between two packing layers

Table 2 lists the geometry of the three tested grids. Using a grid between two packing layers, creates an additional transition zone. The grids with a greater hydraulic diameter than the packing always showed the start of loading and subsequent flooding above the upper transition zone.

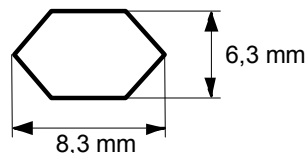
Table 2: list of vane-type elements

- coarse honeycomb



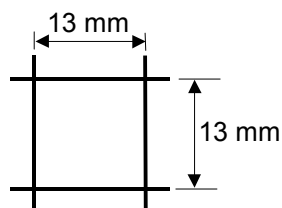
wall thickness : 0,1 mm  
 height : 5 mm  
 material : aluminium

- fine honeycomb



wall thickness : 0,064 mm  
 height : 10 mm  
 material : aluminium

- coarse lattice



wall thickness : 0,5 mm  
 height : 12 mm  
 material : aluminium



A second series of tests was made with height-staggered sheets as shown in Figure 5 and with flattened edges on the bottom side, on the top side and on both sides as shown in Figure 6a. Tests according to this layout have been reported by Billingham and Lockett [3] (Praxair patent application [10]).

With a height-staggered layout, the flow channel circumference is reduced by a factor 2 in the lower part of the sheets and with the flattened edges by a factor 1.45. A greater hydraulic diameter follows from the reduced flow channel circumference and so the effective gas velocity is reduced.

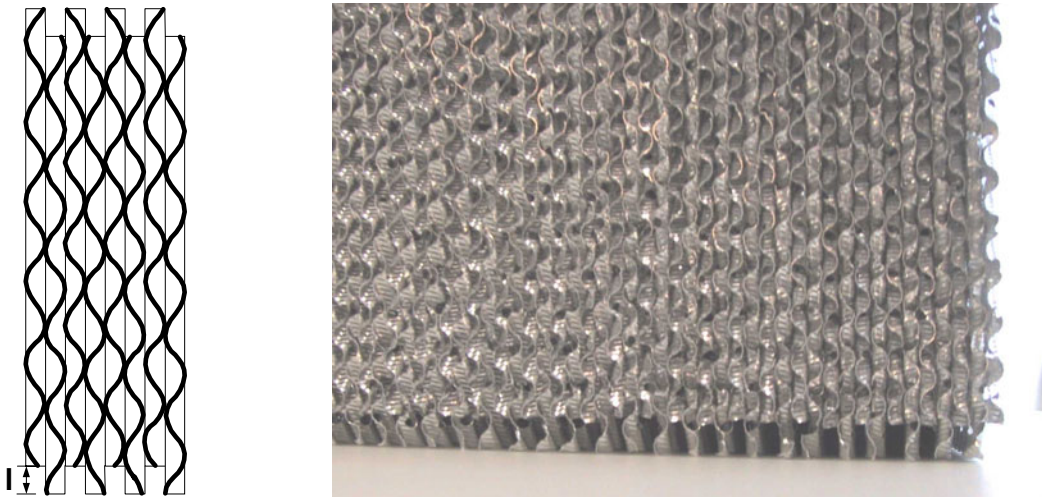


Figure 5: Height-staggered layout of the packing sheets ( $l=10\text{mm}$ )

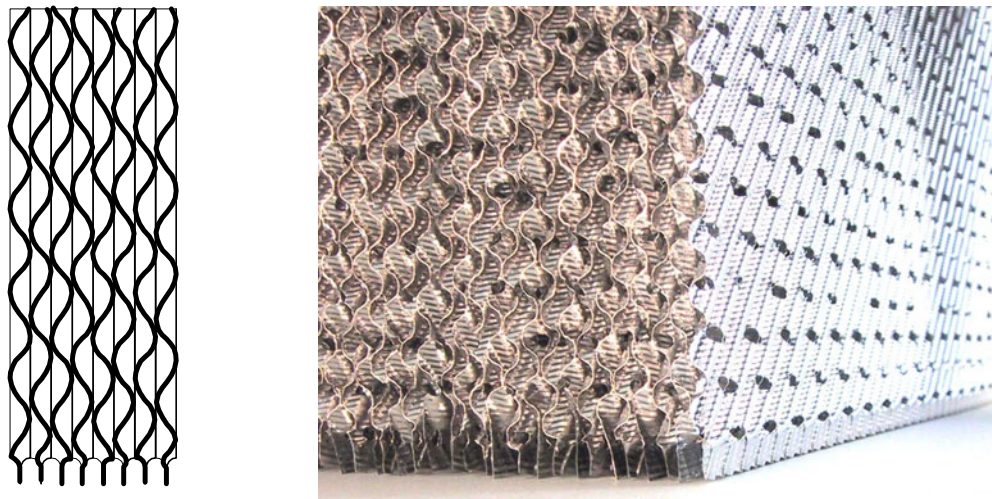


Figure 6a: Packing sheets with flattened edges at the bottom side.

During the production process of the flattened part by squeezing, a sawtooth is formed on the edge. The corrugation form influences the appearance of the flattened edge as can be seen in Figure 6b. The sawtooth form on the edge is very uniform for type A750Y. The tips of the small teeth form a straight line. The teeth of A750Y-PA are more uneven.

Two types of packing with flattened edges have therefore been produced from the two slightly different packing types A750Y and A750Y-PA.

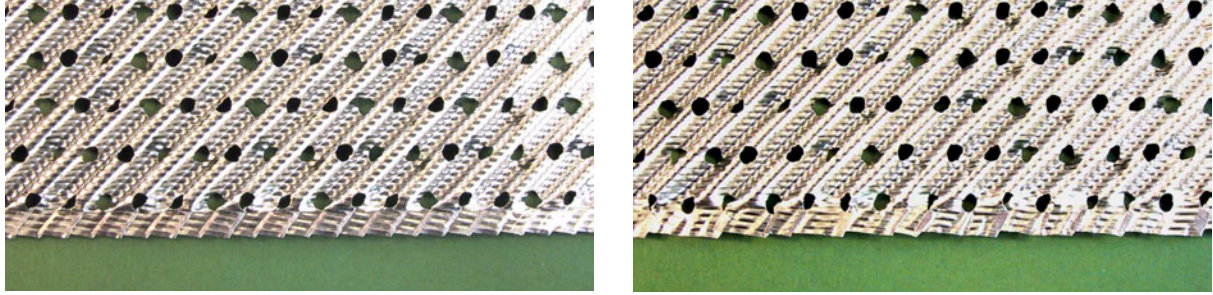


Figure 6b: The edges of the flattened parts of two different A750Y-types. On the left, the edge is covered very uniformly with teeth of uniform size. This sheet is produced from A750Y. The tips are in a straight line. On the right, the teeth have different sizes and form a more uneven edge. The corrugation form corresponds to A750Y-PA.

The effective velocity  $u_{g,eff}$  in the flow channel depends also on the angle of corrugation.

$$u_{g,eff} = \frac{u_g}{\varepsilon * \sin(\alpha)} \quad (2)$$

Increasing  $\alpha$  leads to a smaller effective velocity in the gas channel. Therefore, in a third series, we tested packing sheets in which the corrugations are bent to the vertical on the bottom and top sides as pictured in Figure 7 (Sulzer patent application [11]). We also tested sheets where the corrugations are bent to the vertical only at the bottom side (Montz patent application [12]) and sheets with this bend at the top side only.

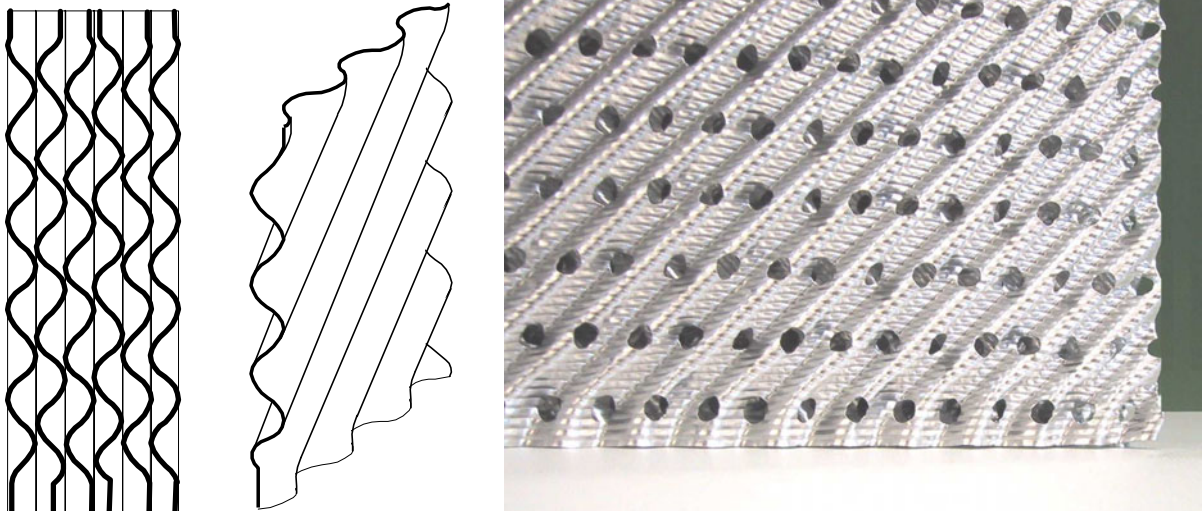


Figure 7: Packing sheets with a bend of the corrugation at the bottom side. The almost vertical part of the bend is about 3mm high. The 45° inclination angle is reached in a height of about 10mm.



## TEST RESULTS

### Vane type spacers

Figure 8 shows the effect of vane type element spacers between the packing layers. The hydraulic diameter of all three spacers tested is greater than the hydraulic diameter of the A750Y. The capacity seems to increase with increasing height of the different spacers.

Olujic at al. [2] made similar tests with a Montz packing B1-250 using short vertical elements of this packing as spacer (air/water,  $D=0.45\text{m}$ ,  $1.013\text{bar}$ , liquid load= $10\text{m}^3/\text{m}^2\cdot\text{hr}$ ). Even though the pressure drop with spacer was lower, the capacity decreased slightly.

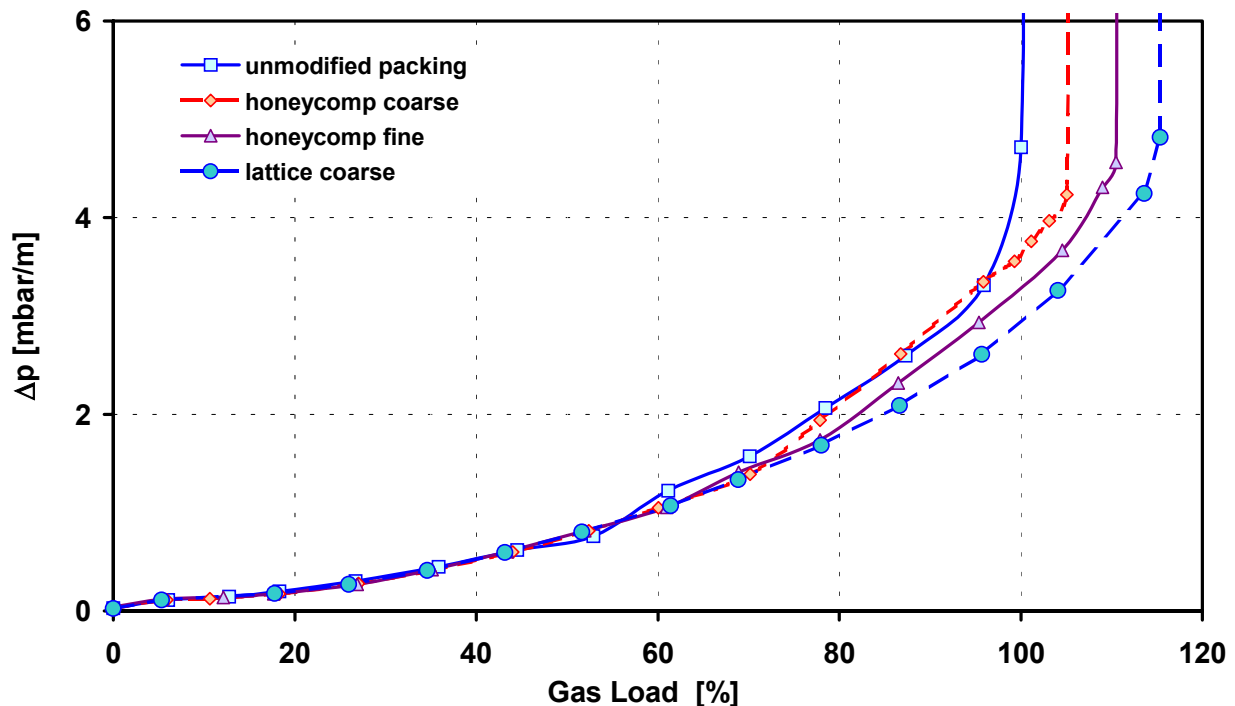


Figure 8: Pressure drop as function of gas load for the unmodified packing and three different vane type elements used as spacers. The liquid load is  $8\text{m}^3/\text{m}^2\cdot\text{hr}$ . The achieved gas load of the unmodified packing at incipient flooding is set to 100%. The height of the coarse honeycomb element is 5mm, the fine honeycomb element is 10mm high and the coarse lattice element is 12mm height.

The reason for this slight decrease in capacity is not yet understood. In their experiment the sheets of the short vertical spacer are oriented parallel to the sheets above. This reduces the number of contact points/ $\text{m}^2$  from  $1/h^2$  to approximately  $2/(b\cdot h)$ . (The corrugation base length,  $b$  is normally greater than twice the corrugation height,  $h$ ). However, the number of contact points in our experiments is even lower without reducing the capacity.

Billingham and Lockett [3] measured a slight decrease in pressure drop with an aluminium packing Koch Flexipac type 1Y ( $420\text{m}^2/\text{m}^3$ ) by installing a gap between the layers (as can be seen in their Figure 2), but no change in capacity (air/water:  $D=0.305\text{m}$ , liquid load =  $23\text{m}^3/\text{m}^2\cdot\text{hr}$ ).

### Height-staggered layout and influence of void fraction

In Figure 9, the effect of void fraction and height staggered layout is shown. The measured increase in the gas load factor  $F_G$  and in the capacity for the sheets with reduced thickness is 8%. The change in void fraction is only 2.7%. The increase is higher than expected from Verschoof's correlation. With height-staggered layout the capacity increased 38%.

Billingham and Lockett [3] tested the influence of the height staggered layout. For the Koch Glitsch packing type 1Y ( $420 \text{ m}^2/\text{m}^3$ ) they found a capacity increase of about 38% ( $D = 0.305\text{m}$ , air-water, liquid load =  $23\text{m}^3/\text{m}^2\cdot\text{hr}$ ) with a staggered height of 6 and 13mm.

They also tested a 750Y packing. With 13mm staggered-height and a liquid load of  $12.3\text{m}^3/\text{m}^2\cdot\text{hr}$ , they obtained an increase of approximately 45% in air-water tests. Experiments with the same packing layout in a series of cryogenic distillation tests ( $D = 0.305\text{m}$ , 1.5bar, total reflux, oxygen-argon mixture) only resulted in a capacity increase of 15% compared with tests using the unmodified packing. This small capacity increase compared with their air-water tests and our results is unexpected.

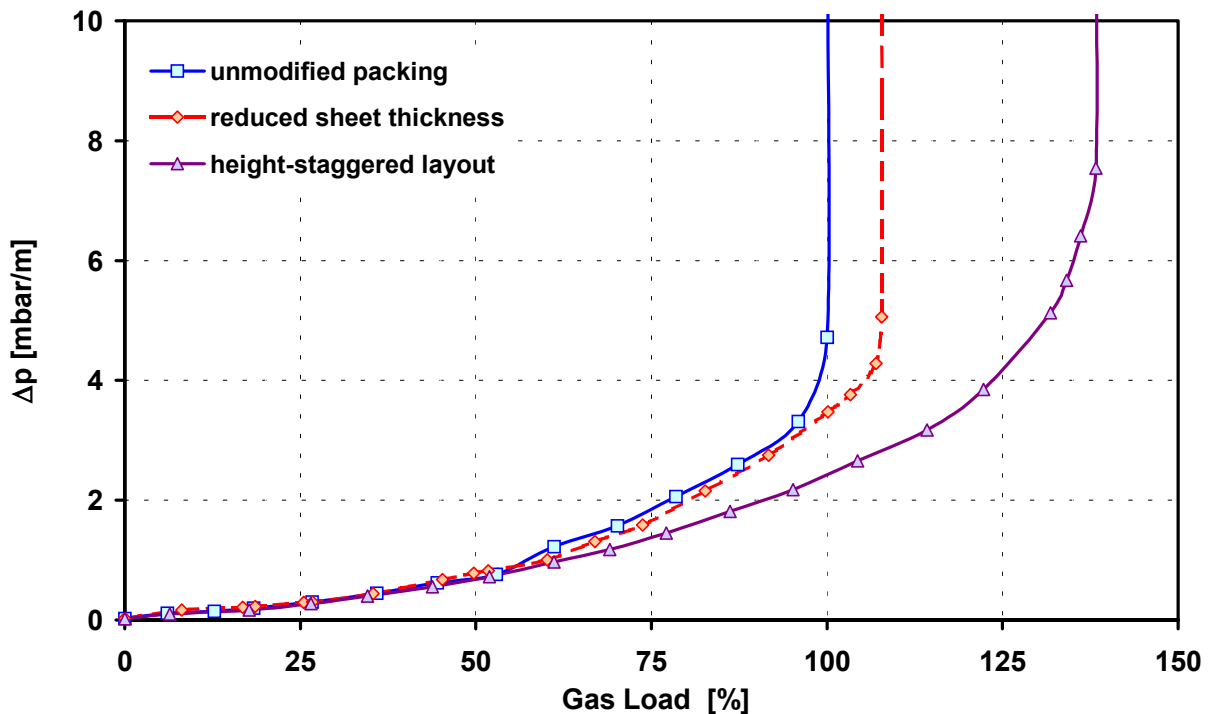


Figure 9: Pressure drop curves for a packing with 95% void fraction instead of 92.5% for the non-modified packing and a pressure drop curve for a 10mm height-staggered layout. The liquid load is  $8\text{m}^3/\text{m}^2\cdot\text{hr}$ . The achieved gas load of the unmodified packing at incipient flooding is set to 100%.

### Flattened edges

Figure 10 shows that a flattened edge on the top side has almost no effect on the capacity achieved when compared with the unmodified packing. The flattened edge on the bottom side of the sheets increases the capacity by more than 50%. This was the highest capacity increase achieved of all packing modifications tested. Even with flattened edges, however, the flooding was observed to start at the bottom side of the layers. This means that there is perhaps a potential for further capacity increase.

Sheets with a flattened edge on the top side show an almost identical pressure drop to sheets with an unmodified top side. Because the flat top edges are parallel to the gas flow direction on the top side, the flow direction change at the entrance to the flow channels of the sheets above is hardly influenced. The strong influence of the direction change at the top edge of the sheets can be seen in Figure 12 where the smaller pressure drop for sheets with corrugations bent to the vertical on the top side is depicted.

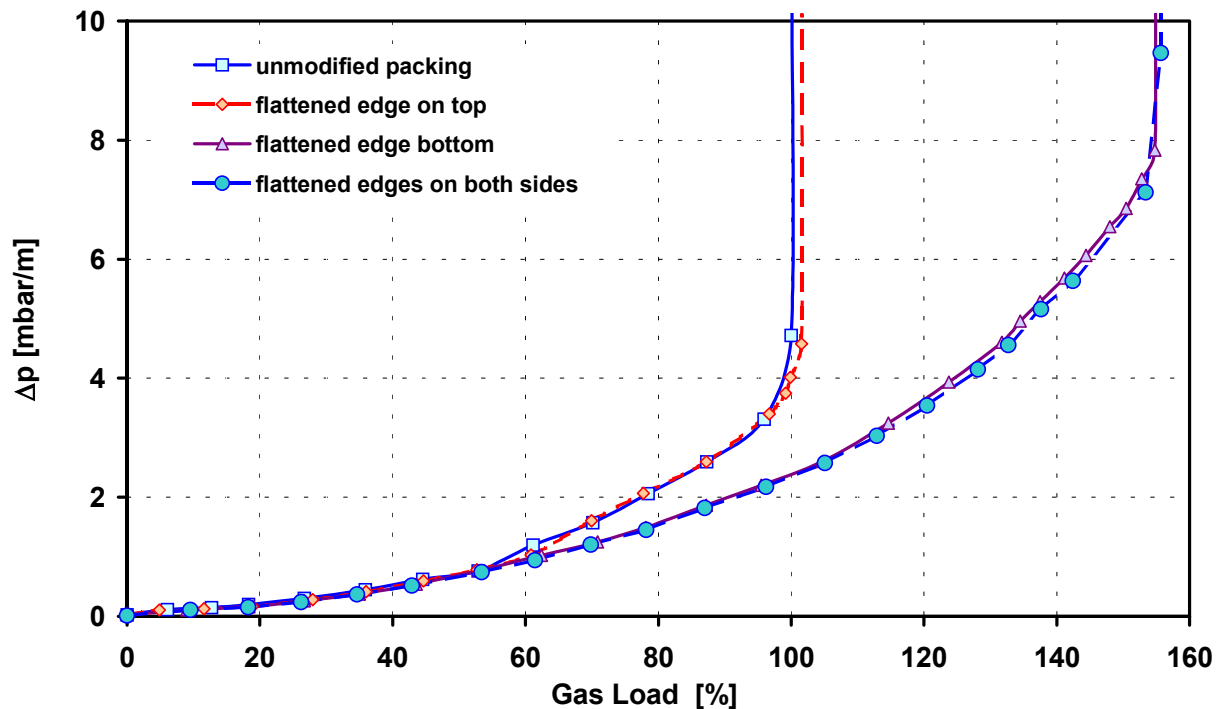


Figure 10: Packing with flattened edge on the top side of the sheets, on the bottom side and on both sides of the sheets. The liquid load is  $8\text{m}^3/\text{m}^2\cdot\text{hr}$ . The achieved gas load of the unmodified packing at incipient flooding is set to 100%. The edges of the flattened parts are covered very uniformly with sawtooths, formed during the production of the flat part of the sheet by squeezing.

The capacity increase is even greater with flattened edges than with height-staggered sheets. That probably signifies that with height staggered sheets only a part of the liquid from the higher positioned sheets flows smoothly to the neighbouring sheets with the lower positioned edges. Liquid builds up at the lower edge of the higher positioned sheets.

Figure 11 demonstrates the effect of the corrugation form. This form influences the vortices in the gas flow and the interaction of gas streams at open crossings of the gas flow channels. Above the loading point the pressure drop of the unmodified packing A750Y-PA shows a steeper increase than the unmodified A750Y, while flooding occurs at a 5% higher load.

The packing A750Y-PA with the flattened edges at the bottom side has a similar performance. The gradient of the pressure drop curve above the loading point is much steeper than the gradient of the A750Y with flattened edges. However, the slope is also much steeper than the gradient of the unmodified A750Y-PA above the loading point. This is different to the packing with bends in the corrugation as can be

seen in Figure 12. This gradient above the loading point is approximately the same for the unmodified and modified packings.

We presume that the reason for this performance at lower liquid loads is the uneven lower edge. The number of contact points between the sheets above and below is reduced. With higher liquid loads, the capacity increase compared with an unmodified A750Y-PA is much higher and reaches about 50% (Figure 13). It is probable that small gaps between the contact points are bridged by the thicker liquid film.

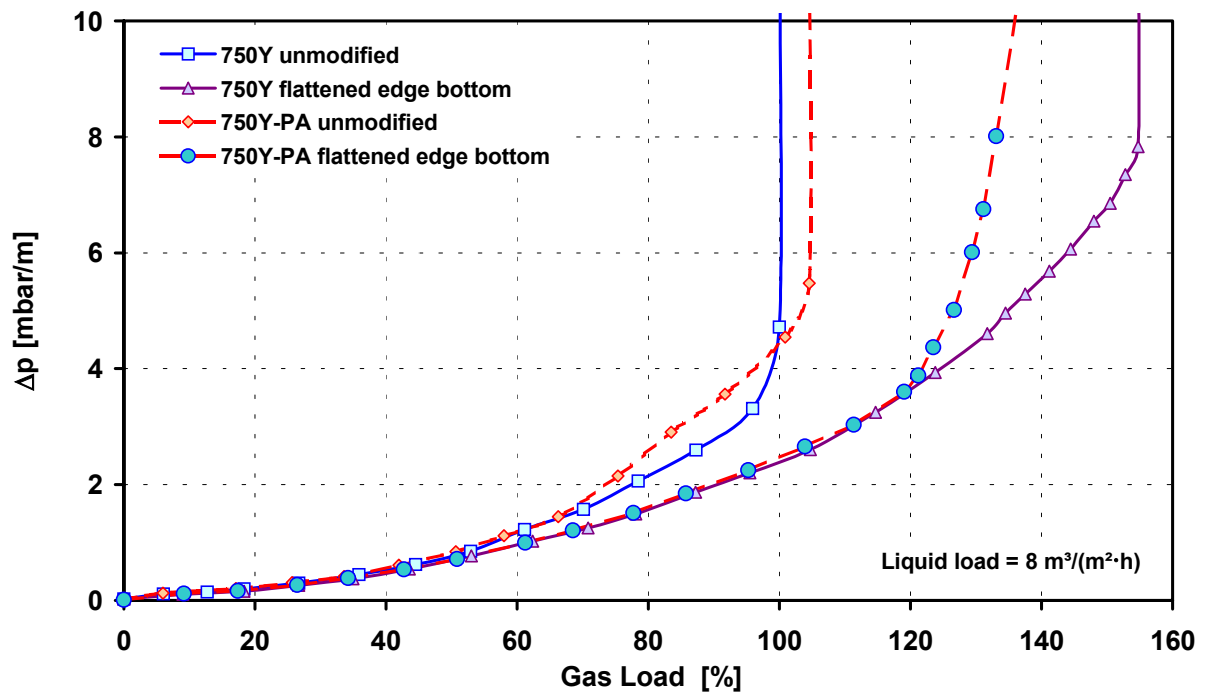


Figure 11: Pressure drop curves as a function of the gas load for sheets with flattened edges on the bottom side for packings of type A750Y and A750Y-PA. The achieved gas load of the unmodified packing at incipient flooding is set to 100%. The capacity advantage for the type A750Y-PA is limited to 39% related to A750Y unmodified.

McNulty and Sommerfeldt [1] investigated in detail their Koch-Glitsch Flexipac HC type 1Y ( $420 \text{ m}^2/\text{m}^3$ ). This packing differs from the conventional Flexipac only in the flattened bottom edge. They found that the capacity advantage decreases from about 44% advantage at very low liquid loads to no capacity difference at liquid loads higher than  $120 \text{ m}^3/\text{m}^2 \cdot \text{hr}$ . They also measured the capacity gain in several other types. With increasing corrugation height (decreasing specific surface area) and increasing liquid load, the advantage decreases to about 15% for type 2Y ( $220 \text{ m}^2/\text{m}^3$ ).

They also tested a Flexipac HC type 700Y in a hydrocarbon test facility. In distillation tests with p/o xylene, the capacity increase compared with that in a conventional packing was 27% ( $D=0.2\text{m}$ , 1.6bar, total reflux, liquid load about  $20 \text{ m}^3/\text{m}^2 \cdot \text{hr}$ ). The same packing showed in air water tests an advantage of only 15% ( $D=0.91\text{m}$ ). The difference is not explained by the authors.

## Bend in the corrugations

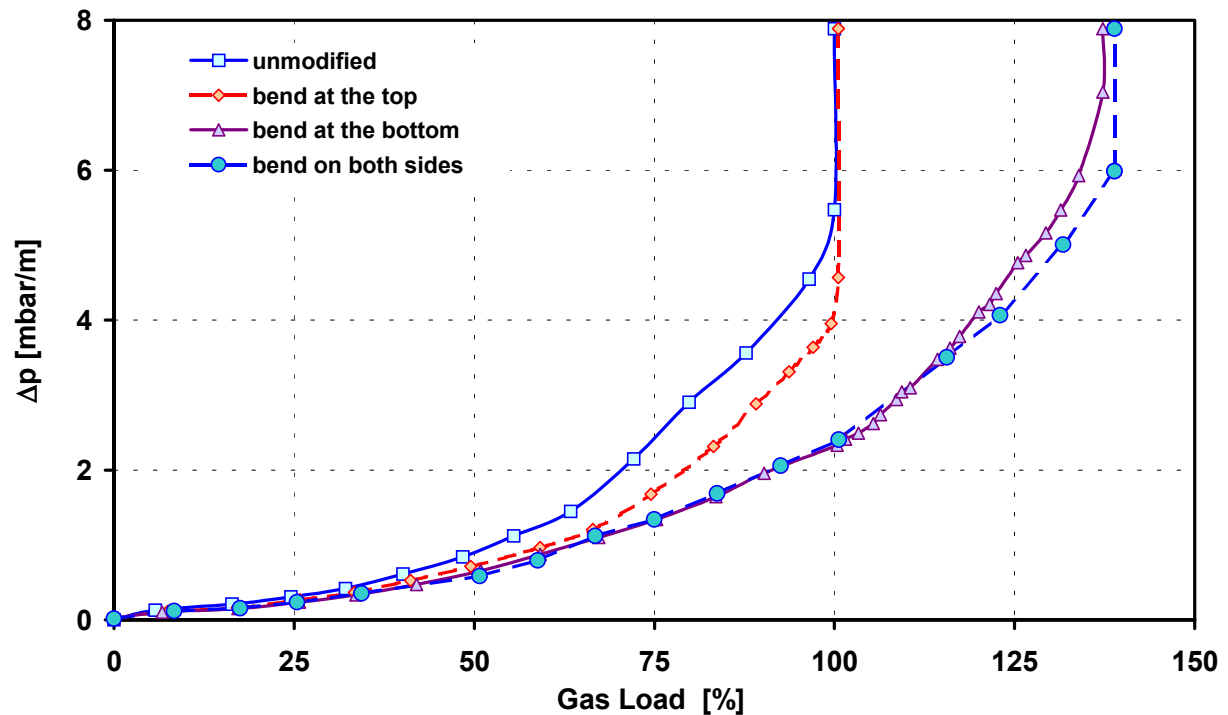


Figure 12: Pressure drop curves as a function of the gas load for sheets, in which the corrugation is bent to the vertical at the top side, at the bottom side and on both sides of the sheets. The curve for an unmodified packing A750Y-PA is also shown, with is the starting material.

In Figure 12 the pressure drop curves with a bend at the top, bottom and both sides are compared with the unmodified packing A750Y-PA.

Remarkable is the form of the curves. With the bend on the top side, the pressure drop increase, starting at the loading point, is smaller than without a bend on the top side. This is probably caused by a smaller change in the gas flow direction at the entrance to the flow channels of the sheets above. The same effect is observed in Figure 8 with vane type elements as spacer between the bricks.

The form of the curve with one bend at the top side is similar to the measured pressure drop curve of Olujic [2] (his Fig. 11) with a short vertical packing between the normal packing layers. The capacity increase achieved compared with the increase using flattened edges is smaller. The circumference of the flow channels at the bottom side is about 40% longer than those with flattened edges. The area of the liquid film offered to the shearing force caused by the gas flow is therefore much higher.

The bend of the corrugation is relatively small when compared with that of a Sulzer Mellapak Plus or Montz B1-M. Capacity increases achieved between the test pair M752.Y and A500Y and the measured increase of a M252.Y to a M250.Y of approximately 34 - 45% in vacuum down to 18% at 1.65bar (FRI [13]) were comparable with our measurements. We therefore conclude that our small bend has the same effect.



## Influence of liquid load

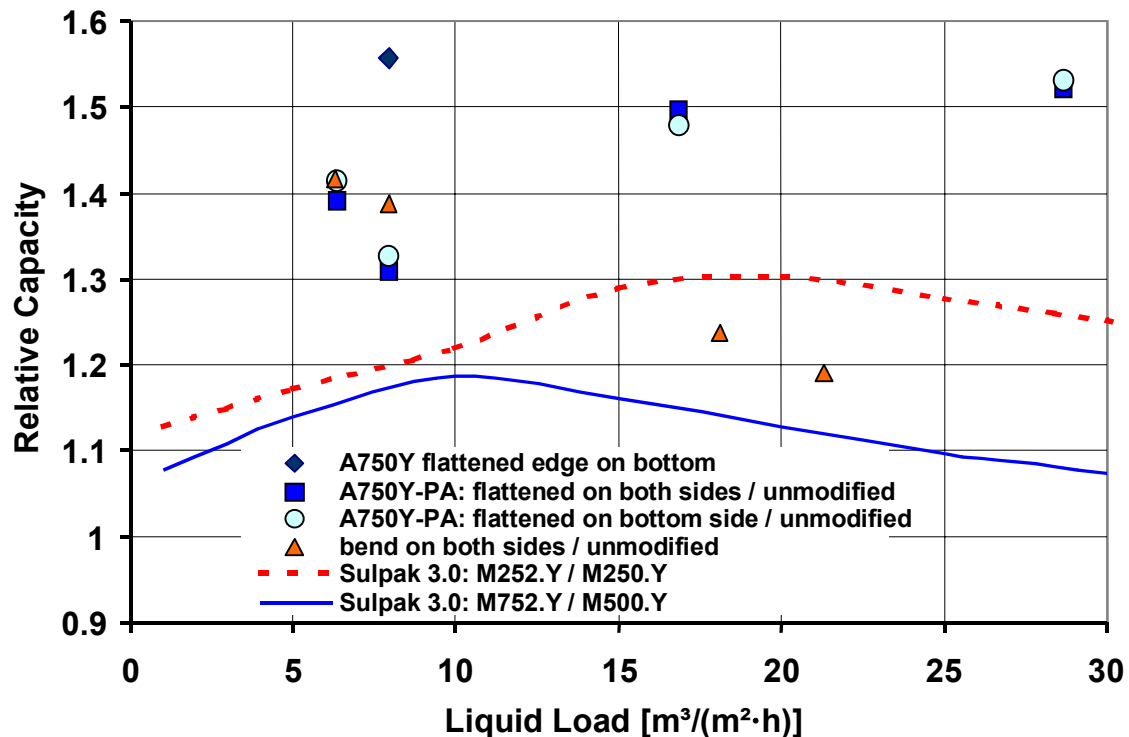


Figure 13: Influence of the liquid load on the attainable relative capacity increase for uneven flattened edges at the bottom and on both sides of the sheets and for sheets with curved corrugations at both sides. These values are compared to the calculated ratio of a M752.Y to a M500.Y and a M252.Y compared to a M250.Y. The calculations are done with the Sulzer program SULPAK 3.0.

Figure 13 shows the influence of the liquid load to the capacity advantage for some modifications of the packing. The highest capacity increase is reached with flattened edges – also for quite high liquid loads.

The advantage of a A750Y with flattened edges at a liquid load of  $8\text{m}^3/\text{m}^2\cdot\text{hr}$  over a 750Y-PA is probably caused by a very uniform and even lower edge. The even edge generates more contact points between the layers.

### Summary table

Table 3 shows the evaluated packings and their modifications. The liquid load of these investigations was  $8\text{m}^3/\text{m}^2\cdot\text{hr}$ .

Table 3: Packings investigated and capacity increases achieved

experiment No.	spec. surface/angle/ sheet thickness [m <sup>2</sup> /m <sup>3</sup> ] / [°] / [mm]	modification	capacity increase (at 8m <sup>3</sup> /m <sup>2</sup> ·hr liquid load)
1	750 / 45 / 0.2	basis of evaluation	100 %
2	750 / 45 / 0.2	coarse lattice*	104 %
3	750 / 45 / 0.2	coarse honeycomb*	111 %
4	750 / 45 / 0.2	fine honeycomb*	115 %
5	750 / 45 / 0.2	flattened edge on top side (h=12mm)	102 %
6	750 / 45 / 0.2	flattened edge on bottom side (h=12mm)	154 %
7	750 / 45 / 0.2 form PA	flattened edge on bottom side (h=12mm)	139 %
8	750 / 45 / 0.2	height staggered composition (h=10mm)	138 %
9	750 / 45 / 0.15	metal sheet thickness reduced	108 %
10	750 / 45 / 0.2	corrugation angle on bottom side	137 %
11	750 / 45 / 0.2	corrugation angle on top side	101 %
12	750 / 45 / 0.2	corrugation angle on both sides	139 %
* see also precise description above			

## Conclusion

The basis of our tests was a Linde aluminium packing A750Y with a specific surface area  $a$  of 750m<sup>2</sup>/m<sup>3</sup>, a sheet thickness of 0.2mm and a corrugation angle of 45°. The comparisons of the different modifications have been conducted with a liquid load of 8m<sup>3</sup>/m<sup>2</sup>·h. The highest capacity increase of about 55% was achieved with flattened edges of the packing sheets. Height-staggered sheets and sheets, in which the corrugations at the bottom and top side are bent to the vertical showed an increase in capacity of about 38%.

While the use of the modifications at the top side only reduced the pressure drop but did not enhance the capacity, these tested modifications resulted in a substantial capacity increase.

Using a grid between the unmodified packing layers lowered the pressure drop and gave a capacity increase of up to 15% with increasing grid height. The hydraulic diameter of the grids tested was more than twice as large as the hydraulic diameter of the packing.

All the packing modifications tested started to flood immediately above the transition zone between two layers. We conclude therefore that the capacity in the core of the packings is higher than 155%. The occurrence of a loading point is caused by a insufficient drainage at the lower edge of the packing sheets and by an imperfect incoming gas flow. The measured shift to higher capacity caused by the modifications tested was accompanied by an similar shift of the loading point.

Distillation tests with argon/oxygen showed that some of the geometries probably tend to generate maldistribution. Reducing this tendency without a penalty in capacity is the goal of further investigations.

## NOMENCLATURE

b	corrugation base length (m)
D	column diameter (m)
$F_G$	gas load factor ( $\text{m/s} \cdot (\text{kg/m}^3)^{0.5}$ )
h	corrugation height (m)
s	sheet thickness (mm)
$u_{g,\text{eff}}$	effective gas velocity in the flow channels (m/s)
$u_{g,s}$	superficial gas velocity (m/s)
$\alpha$	corrugation inclination angle, deg
$\varepsilon$	packing porosity

## REFERENCES

1. Mc Nulty, K.J.; Sommerfeldt, R.A., (1999), New twist adds capacity to Flexipac structured packings, AIChE National Meeting, Houston, March 14-18.
2. Olujic Z., Jansen H., Kaibel B., Rietfort T., Zich E., (2001), Streching the capacity of structured packings, Ind. Eng. Chem. Res., Vol. 40, No. 26, pp. 6172-6180
3. Billingham, J. F.; Lockett, M. J., (1999) Development of a new generation of structured packings for distillation. Trans IChemE, Vol 77, Part A, 583ff
4. P.Suess, L. Spiegel (1992) Hold-up of Mellapack structured packings, Chem Eng Proc, 31. pp.:119-124
5. Zuiderweg F.J., (1994), Fractionation Research Inc., (internal report, ITEM 12, April)
6. Ranke H., Lerzer R., Becker O.; (2000), Hydraulic calculations for cross-channeled packings in distillation units based on a physical model, Chem. Eng. Technol. Vol. 23, No. 8, pp. 691-699
7. Brunazzi E., Paglianti A. (1997) Mechanistic Pressure Drop Model for columns Containing Structured Packings, AIChE Journal, Vol 43, No.2, pp.317-327

8. Ólujic Z. (1997), Development of a Complete Simulation Model for Predicting the Hydraulic and Separation Performance of Distillation Equipped with Structured Packings, Chemical and Biochemical Engineering Q. 11 (1), pp. 31-46
9. Verschoof H.-J., Ólujic Z., Fair J.R. (1999), A general correlation for predicting the load point of corrugated sheet structured packings, Ind. Eng. Chem. Res., Vol. 38, No. 10, pp. 3663-3669
10. European Patent Application, Anmeldeschrift zur Patentierung Nr.: EP 0 707 885 A1 (1996) Structured packing with improved capacity for rectification systems, Praxair Technology, Inc., U.S.A.
11. International Patent Classification Nr.: WO 97/16247 (1997), Structured packing Sulzer Chemtech AG, Winterthur, Schweiz
12. Offenlegungsschrift DE 100 01 694 A1 (2000), Packung für Wärme- und Stoffaustausch, Julius Montz GmbH, 40723 Hilden, DE
13. FRI, (2001), Fractionation Research Inc., (Topical report 141, August 2001)